ELSEVIER

Spectrochimica Acta Part A 56 (2000) 1957–1970

SPECTROCHIMICA ACTA PART A

www.elsevier.nl/locate/saa

Spectra and structure of silicon containing compounds. XXVII [1]. Raman and infrared spectra, conformational stability, vibrational assignment and ab initio calculations of vinyldichlorosilane

Gamil A. Guirgis [2], Pengqian Zhen [3], James R. Durig *

Department of Chemistry, University of Missouri-Kansas City, Kansas City, MO 64110-2499, USA

Received 8 February 2000; accepted 9 March 2000

Abstract

The infrared (3200–30 cm^{-1}) spectra of gaseous and solid and the Raman spectra of liquid (3200 − 30 cm^{-1}), with quantitative depolarization values, and solid vinyldichlorosilane, CH_2=CHSiHCl_2, have been recorded. Both the *gauche* and the *cis* conformers have been identified in the fluid phases. Variable temperature (105–150°C) studies of the infrared spectra of the sample dissolved in liquid krypton have been carried out. From these data the enthalpy difference has been determined to be 20 ± 5 cm^{-1} (235 ± 59 J mol^{-1}) with the *gauche* conformer the more stable rotamer. It was not possible to obtain a single conformer in the solid even with repeated annealing of the sample. The experimental enthalpy difference is in agreement with the prediction from MP2/6-311 + G(2d,2p) ab initio calculations with full electron correlation. However, when smaller basis sets, i.e. 6-31G(d) and 6-311 + G(d,p) were utilized the *cis* conformer was predicted to be the more stable form. Complete vibrational assignments are proposed for both conformers based on infrared contours, relative infrared and Raman intensities, depolarization values and group frequencies, which are supported by normal coordinate calculations utilizing the force constants from ab initio MP2/6-31G(d) calculations. From the frequencies of the Si–H stretches, the Si–H bond distance of 1.474 Å has been determined for both the *gauche* and the *cis* conformers. Complete equilibrium geometries have been determined for both rotamers by ab initio calculations employing the 6-31G(d), 6-311 + G(d,p) and 6-311 + (2d,2p) basis sets at level of Hartree–Fock (RHF) and/or Moller–Plesset to the second order (MP2) with full electron correlation. The potential energy terms for the conformer interconversion have been obtained from the MP2/6-31G(d) calculations. The results are discussed and compared with those obtained for some similar molecules.

Keywords: Spectra; Structure; Silicon containing compounds

* Corresponding author. Tel.: + 1-816-2351136; fax: + 1-816-2355191.

E-mail address: durigj@umkc.edu (J.R. Durig).

[1] For part XXVI, see J. Mol. Struct. (in press).

[2] Present address: Analytical Research and Development Department, Bayer Corp., PO Box 118088, Charleston, SC 29423, USA.

[3] Taken in part from the dissertation of P. Zhen which will be submitted to the Department of Chemistry in partial fulfillment of the PhD degree.

1386-1425/00/$ - see front matter

PII: S1386-1425(00)00254-7

1. Introduction

Vinyldichlorosilane, CH_2=$CHSiHCl_2$, is of scientific interest because of its importance in industry. It has been utilized as a reactant for a wide variety of materials [1–5] and it has been the subject of a vibrational study [6] and theoretical and thermodynamical calculations [7]. In the vibrational analysis of vinyldichlorosilane, it was concluded [6] that the molecule exists in two stable conformers, *gauche* and *cis*, in the liquid phase with an enthalpy difference of 98 ± 10 cm^{-1} (1.17 ± 0.12 kJ mol^{-1}) with the *gauche* conformer the more stable rotamer. Recently, we reported [8] the vibrational and conformational stability of chlorocyclopropylsilane c-$C_3H_5SiH_2Cl$, for which the more stable conformer has been identified to be the *cis* rotamer. This study [8] was carried out to obtain data for comparison with the conformational stability of chlorovinylsilane [9] molecule, which was determined to be stable by 78 ± 11 cm^{-1} (0.93 ± 0.13 kJ mol^{-1}), but with the *gauche* conformation the more stable form. This experimental result [9] was found to be consistent with the predictions from ab initio calculations. In a recent study [10], the vibrational spectrum and conformational stability of dichlorocyclopropylsilane was carried out and it was concluded that this molecule exists in the *gauche* and *cis* conformations in the fluid phases where the *gauche* conformer is the more stable rotamer by 99 ± 7 cm^{-1} (1.18 ± 0.08 kJ mol^{-1}) in xenon solution. This experimental result was also supported by ab initio calculations utilizing different basis sets. Therefore, we initiated the current study of vinyldichlorosilane for the comparison of its stability to that of dichlorocyclopropylsilane because the bonding of the vinyl group is frequently compared with that of the cyclopropyl group.

We have recorded the infrared and Raman spectra of the fluid and solid phases of dichlorovinylsilane. Additionally, we have recorded variable temperature studies of the infrared spectra of the sample dissolved in liquid krypton. We have also carried out ab initio calculations employing a variety of basis sets up to 6-311 + G(2d,2p) at the level of restricted Hartree–Fock (RHF) and/or Moller–Plesset to the second order (MP2) with full electron correlation to obtain complete equilibrium geometries. The harmonic force constants, vibrational frequencies, infrared and Raman intensities and conformational stabilities have also been obtained from MP2/6-31G(d) ab initio calculations. The results of these vibrational and theoretical studies are reported herein.

2. Experimental

The vinyldichlorosilane sample was prepared by the reaction of vinyl silane with excess of tin tetrachloride at room temperature for 18 h. The sample was first purified by trap to trap distillation at reduced pressure and then followed by further purification with a low-temperature and low-pressure fractionation column.

The mid-infrared spectra of the gas and solid (Fig. 1) were obtained from 3200 to 300 cm^{-1} on a Perkin–Elmer model 2000 Fourier transform spectrometer equipped with a Ge/CsI beamsplitter and a DTGS detector. The gas was contained in a 10-cm cell fitted with CsI windows. The spectrum was obtained at a resolution of 0.5 cm^{-1} from 64 co-added scans of the sample and reference and the interferograms transformed with boxcar truncation function. The spectrum of the solid was obtained by condensing the sample onto a boiling liquid nitrogen cooled CsI plate contained in an evacuated cell equipped with CsI windows, and 256 scans were collected for both the reference and sample interferograms at 1 cm^{-1} resolution and then transformed with boxcar truncation function.

The mid-infrared spectra of the sample dissolved in liquified krypton as a function of temperature were recorded on a Bruker model IFS 66 Fourier transform spectrometer equipped with a Globar source, a Ge/KBr beamsplitter and a DTGS detector. In all cases, 100 interferograms were collected at 1.0 cm^{-1} resolution, averaged and transformed with a boxcar truncation function. For these studies, a specially designed cryostat cell was used. It consisted of a copper cell

with a path length of 4 cm with wedged silicon windows sealed to the cell with indium gaskets. The copper cell was enclosed in an evacuated chamber fitted with KBr windows. The temperature was maintained with boiling liquid nitrogen and monitored with two Pt thermoresistors. The complete cell was connected to a pressure manifold, allowing the filling and evacuation of the system. After cooling to the desired temperature, a small amount of the compound was condensed into the cell. Next, the system was pressurized with the noble gas, which immediately started to condense in the cell, allowing the compound to dissolve.

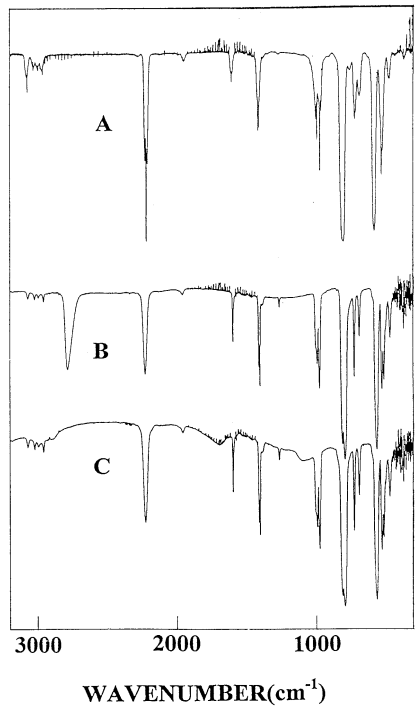

Fig. 1. Mid-infrared spectra of vinyldichlorosilane (A) gas (B) amorphous solid (C) annealed solid.

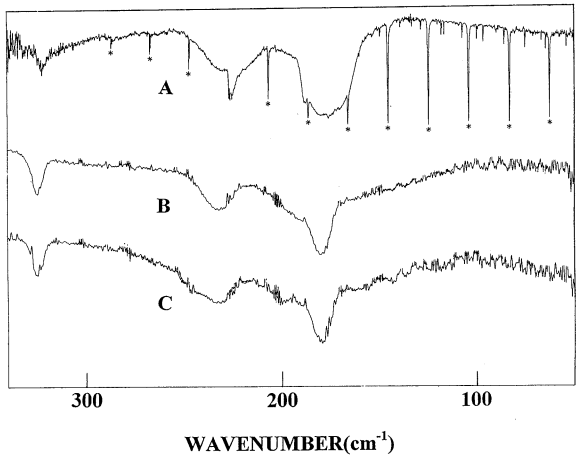

Fig. 2. Far infrared spectra of vinyldichlorosilane (A) gas (B) amorphous solid (C) annealed solid. Sharp bands marked with asterisks are due to HCl impurity on spectrum of the gas.

The far infrared spectrum of the gas (Fig. 2A) was recorded with a Bomem model DA3.002 Fourier transform spectrometer equipped with a vacuum bench, a 6.25 μm Mylar beamsplitter, and a liquid helium cooled Ge bolometer with a wedged sapphire filter and polyethylene window. The spectra were obtained from a sample contained in a 1 m folded path cell equipped with mirrors coated with gold, and fitted with polyethylene windows with an effective resolution of 0.10 cm^{-1}. To remove traces of water, an activated 3 Å molecular sieve was used to dry the sample. Interferograms of the sample and reference were recorded 512 times at a resolution of 0.10 cm^{-1} and transformed with a boxcar truncation function. The spectra of the solids (Fig. 2B and C were obtained with a Perkin–Elmer model 2000 spectrometer equipped with a metal grid beamsplitter and a DTGS detector.

The Raman spectra were recorded on a SPEX model 1403 spectrophotometer equipped with a Spectra-Physics model 164 argon ion laser operating on the 514.5 nm line. The laser power used was 0.5 W with a spectral bandpass of 3 cm^{-1}. The spectrum of the liquid was recorded with the sample sealed in a Pyrex glass capillary held in a Miller–Harney apparatus [11]. Depolarization measurements were obtained for the liquid sample using a standard Ednalite 35 mm camera polarizer with 38 mm of free aperture affixed to the SPEX instrument. Depolarization ratio measurements were checked by measuring the state of polarization of the Raman bands of CCl_4 immediately before depolarization measurements were made on the liquid sample. The measurements of the Raman frequencies are ex-

pected to be accurate to ± 2 cm^{-1} and typical spectra are shown in Fig. 3. All of the observed bands in both the infrared and Raman spectra, along with the proposed assignments, are listed in Table 1.

3. Ab Initio calculations

The LCAO-MO-SCF ab initio calculations were performed with the Gaussian-94 program [12] using Gaussian-type basis functions. The energy minima with respect to nuclear coordinates were obtained by the spontaneous relaxation of all the geometric parameters consistent with the symmetry restrictions using the gradient method of Pulay [13]. The structural optimization for the *gauche* and the *cis* conformers were carried out with initial parameters taken from those of chlorovinylsilane [9]. The 6-31G(d), 6-311 + G(d,p) and 6-311 + G(2d,2p) basis sets were employed at the level of restricted Hartree–Fock and/or Moller–Plesset (MP2) by the perturbation methods to second order with full electron correlation and the determined structural parameters are listed in Table 2.

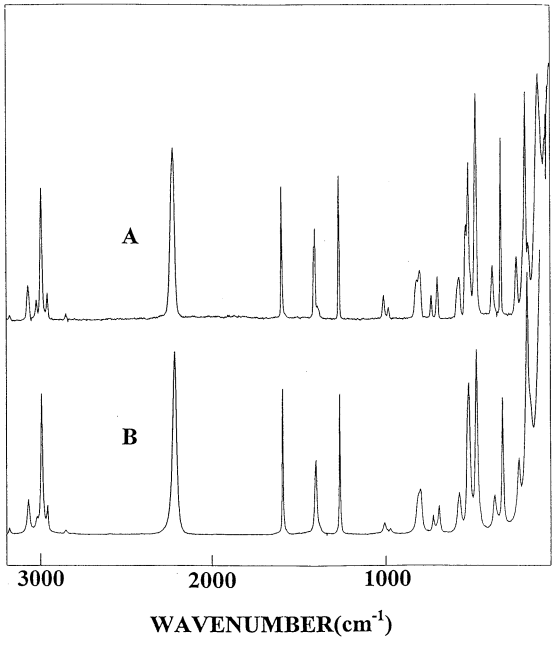

Fig. 3. Raman spectra of vinyldichlorosilane (A) liquid (B) annealed solid.

We have carried out normal coordinate analysis of vinyldichlorosilane. The force fields in Cartesian coordinates were calculated by the Gaussian-94 program [12] with the MP2/6-31G(d) basis set. The internal coordinates (Fig. 4) were used to calculate the G and B matrices utilizing the structural parameters given in Table 2. Using the B matrix [14], the force field in Cartesian coordinates was converted to a force field in internal coordinates, and the pure ab initio vibrational frequencies were reproduced. The force constants for both the *gauche* and *cis* conformers can be obtained from the authors. Subsequently, scaling factors of 0.9 for stretching and bending and 1.0 for the torsional coordinates, and the geometric average of scaling factors for interaction force constants were used to obtain the fixed scaled force field and resultant wavenumbers. A set of symmetry coordinates was used (Table 3) to determine the corresponding potential energy distributions (P.E.D.). A comparison between the observed and calculated frequencies of vinyldichlorosilane along with the calculated infrared intensities, Raman activities, depolarization ratios and P.E.D. are given in Table 4.

Raman and infrared spectra for vinyldichlorosilane were calculated using the predicted frequencies, scattering activities and infrared intensities determined from the ab initio calculations. The Gaussian-94 program [12] with the option of calculating the polarizability derivatives [RHF/6-31G(d)] was used. The evaluation of the Raman activity by using the analytical gradient methods has been developed [15,16]. The activity S_j can be expressed as:

$$S_j = g_j(45\alpha_j^2 + 7\beta_j^2)$$

where g_j is the degeneracy of the vibrational mode j, α_j is the derivative of the isotropic polanizability, and β_j is that of the anisotropic polarizability. The Raman scattering cross-sections, $\partial\sigma_j/\partial\Omega$, which are proportional to the Raman intensities, can be calculated from the scattering activities and the predicted frequencies for each normal mode using the relationship [17,18]:

Table 1
Observed[a] infrared and Raman wavenumbers (cm^{-1}) for vinyldichlorosilane

Gas	Infrared					Raman				Assignment	
	Rel. int.	Kr soln.	Rel. int.	Solid	Rel. int.	Liquid	Rel. int. and depol.	Solid	Rel. int.	ν_i[b]	Approximate description
3084 R											
3079 Q, A/C	w	3076	vw							ν_1	CH_2 antisymmetric stretch
3074 Q	w	3069	vw	3071	vw	3071	w, p	3070	w	ν'_1	
3066 P											
3035 R											
3030 Q	w	3024	vw	3021	vw	3021	vw, p	3020	vw	ν'_3	or $(\nu_4+\nu_9)$
3023 P											
3006 R											
3001 min B	w	2994	vw	2994	vw	2992	m, p	2992	m	ν_2	CH_2 symmetric stretch
2995 P											
2965 max	w	2960	vw	2956	w	2956	vw, p	2955	vw	ν'_2, ν_3	CH stretch
2247 R											
2219 Q, A/C	vs	2217	m	2228	m	2217	s, p	2225	s	ν_4, ν'_4	Si–H stretch
2218 sh											
2210 P											
1608 R											
1603 Q, A/C	w	1599	w	1595	w	1595	m, p	1594	m	ν_5, ν'_5	C=C stretch
1597 P											
1418 R											
1413 Q	m	1410	m	1409	m			1407	w	ν_6	CH_2 deformation
1407 Q, C	m	1403	m	1402	s	1402	w, p	1400	m	ν'_6	
1402 P											
1276 R											
1272 Q, A/C	vw	1274	m	1264	vw	1265	m, p	1263	s	ν_7, ν'_7	CH in-plane bend
1269 Q											
1265 P											
1004 max	m	1006	w	1004	sh, m	1008	bd, vw, p	1006	vw	ν_8, ν'_8	CH_2 wag
997 Q	m	998	m	996	m	999	sh, vw, dp			ν_9, ν'_9	CH_2 twist
		995 m									
986 R											
977 Q, A/C	s	975	s	980	s	973	vw, dp	977	vw	ν_{10}	CH_2 wag
973 Q	m	971	m							ν'_{10}	
969 P											
828 R											

Table 1 (*Continued*)

Gas	Infrared					Raman				Assignment	
	Rel. int.	Kr soln.	Rel. int.	Solid	Rel. int.	Liquid	Rel. int. and depol.	Solid	Rel. int.	ν_i[b]	Approximate description
824 Q	vs	821	vs	814	vs	811	sh, w, p	812	sh, w	ν_{11}	SiH in-plane bend
810 max	vs	805	vs	797	vs	800	w, p	796	w	ν'_{11}, ν_{12}, ν'_{12}	SiH bend
734 R											
730 Q, A/C	m	730	m	732	s	726	vw, p	728	vw	ν'_{13}	
723 P											
697 R											
694 Q, A/C	w	695	w	696	w	692	w, p	694	w	ν_{13}	Si–C stretch
689 P											
589 max	vs	585	vs	568	vs	574	w, dp	569	w	ν_{14}, ν'_{14}	$SiCl_2$ antisymmetric stretch
542 R											
536 Q, A/C	s	534	m	532	s	525	sh, m, p	530	m	ν_{15}	CH out-of-plane bend
531 Q		528	m	518	s	519	s, p	515	s	ν'_{16}	
529 P				505	sh, w			504	sh	ν'_{15}	
482 max	bd, w	480	w	475	w	475	s, p	471	vs	ν_{16}	$SiCl_2$ symmetric stretch
371 max	bd, w			378	w	367	w, p	374	w	ν_{17}	SiC=C bend
322 max	vw			325	vw	321	m, p	323	s	ν'_{17}	
231 R											
226 Q	w			232	vw	225	w, p	229	w	ν_{18}	$SiCl_2$ wag
218 P				189	sh, vw			187	w	ν'_{18}	
175 max	bd, w			179	w	175	vs, p	177	vs	ν_{19}, ν'_{19}, ν'_{20}	$SiCl_2$ deformation
						156	sh, m, p	162	w	ν_{20}	$SiCl_2$ rock
								103	s	ν_{21}, ν'_{21}	Asymmetric torsion

[a] Abbreviations used: s, strong; m, moderate; w, weak; v, very; bd, broad; sh, shoulder; p, polarized; dp, depolarized; A, B and C refer to infrared band envelopes; P, Q and R refer to the rotational vibrational branches.

[b] ν_i and ν'_i refer to the *gauche* and *cis* conformers, respectively.

$$\frac{\partial\sigma_j}{\partial\Omega}=\left(\frac{2^4\pi^4}{45}\right)\left(\frac{(v_0-v_j)^4}{1-\exp\left[\frac{-hcv_j}{kT}\right]}\right)\left(\frac{h}{8\pi^2cv_j}\right)S_j$$

where v_0 is the exciting frequency, v_j is the vibrational frequency of the jth normal mode, h, c and k are universal constants, and S_j is the corresponding Raman scattering activity. To obtain the polarized Raman scattering cross-section, the polarizabilities are incorporated into by S_j by $S_j[(1-\rho_j)/(1+\rho_j)]$ where ρ_j is the depolarization ratio of the jth normal mode. The Raman scattering cross-sections and calculated fixed scaled frequencies were used together with a Lorentzian line shape function to obtain the calculated spectrum. The predicted Raman spectra of the pure *cis* and *gauche* conformers are shown in Fig. 5C and D, respectively. The predicted Raman spectrum of the mixture of the two conformers with a ΔH value of 20 cm^{-1} (experimental value, see conformational stability) is shown in Fig. 5B which should be compared with the experimental spectrum of the liquid (Fig. 5A). The predicted intensities for the C=C stretch, the CH_2 deformation, and CH bend are much smaller than the

Table 2
Structural parameters[a], rotational constants, dipole moments and energy for vinyldichlorosilane

Parameter	RHF/6-31G(d)		MP2/6-31G(d)		MP2/6-311+G(d,p)		MP2/6-311+G(2d,2p)	
	Gauche	*Cis*	*Gauche*	*Cis*	*Gauche*	*Cis*	*Gauche*	*Cis*
rSiH	1.461	1.461	1.476	1.476	1.465	1.467	1.459	1.461
rC_3Si	1.853	1.849	1.847	1.842	1.846	1.841	1.841	1.836
rC_4C_3	1.325	1.326	1.343	1.344	1.347	1.347	1.339	1.339
$rSiCl_5$	2.060	2.059	2.051	2.050	2.048	2.047	2.060	2.059
$rSiCl_6$	2.057	2.059	2.048	2.050	2.046	2.047	2.058	2.059
rC_3H_7	1.080	1.079	1.090	1.089	1.091	1.089	1.083	1.081
rC_4H_8	1.077	1.077	1.087	1.087	1.087	1.087	1.080	1.080
rC_4H_9	1.075	1.077	1.089	1.087	1.087	1.088	1.079	1.081
$\angle C_3SiH$	113.5	111.5	113.5	110.5	113.6	110.6	114.0	111.1
$\angle C_4C_3Si$	125.1	121.3	124.1	120.2	124.2	120.7	123.9	120.4
$\angle HSiCl_5$	106.6	108.1	106.9	108.5	107.0	108.6	106.8	108.6
$\angle HSiCl_6$	107.4	108.1	107.6	108.5	107.8	108.6	107.7	108.6
$\angle Cl_5SiC_3$	109.5	110.6	109.2	110.6	109.2	110.4	109.1	110.4
$\angle Cl_6SiC_3$	110.7	110.6	109.9	110.6	109.9	110.4	109.8	110.4
$\angle H_7C_3Si$	116.4	119.6	117.3	120.6	117.5	120.3	118.0	120.7
$\angle H_8C_4C_3$	121.6	122.0	121.8	122.2	121.5	121.9	121.5	121.9
$\angle H_9C_4C_3$	122.5	122.3	121.9	121.9	121.7	121.6	121.5	121.5
τC_4C_3SiH	118.6	0.0	117.1	0.0	118.2	0.0	117.3	0.0
τCl_5SiHC_3	−120.7	121.7	−120.5	121.2	−119.3	120.2	−120.6	121.5
τCl_6SiHC_3	122.2	−121.7	121.9	−121.2	120.9	−120.2	122.1	−121.5
$\tau H_7C_3SiC_4$	180.0	180.0	180.0	180.0	180.0	180.0	180.0	180.0
$\tau H_8C_4C_3Si$	180.0	180.0	180.0	180.0	180.0	180.0	180.0	180.0
$\tau H_9C_4C_3H_8$	180.0	180.0	180.0	180.0	180.0	180.0	180.0	180.0
A	2699	2410	2750	2413	2749	2425	2751	2411
B	1981	2044	1979	2059	1985	2056	1975	2057
C	1259	1189	1271	1195	1276	1198	1271	1194
$\lvert\mu_a\rvert$	1.921	3.131	1.834	3.053	1.712	2.843	1.554	2.629
$\lvert\mu_b\rvert$	2.012	0.000	1.974	0.000	1.785	0.000	1.689	0.000
$\lvert\mu_c\rvert$	0.831	0.484	0.785	0.428	0.763	0.493	0.596	0.345
$\lvert\mu_t\rvert$	2.903	3.168	2.806	3.083	2.588	2.885	2.371	2.652
$-(E+1280)$	6.03301	6.03365	6.65788	6.65833	6.77323	6.77349	7.15130	7.15117
ΔE (cm^{-1})	140		99		57		30	

[a] Bond distances in Å, bond angles in degrees, rotational constants in MHz, dipole moments in Debye and energies in Hartrees.

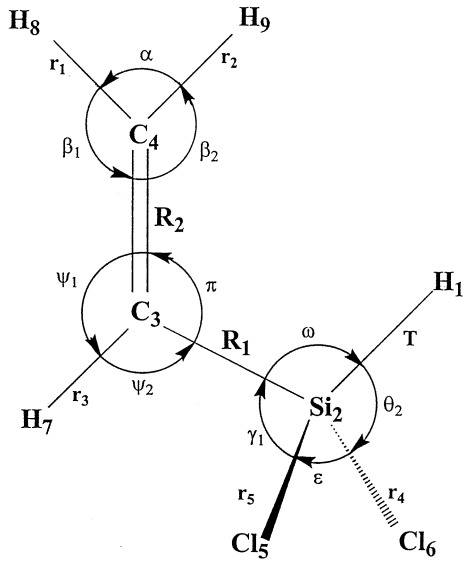

Fig. 4. Internal coordinates of vinyldichlorosi lane.

Table 3
Symmetry coordinates for vinyldichlorosilane

CH_2 antisymmetric stretch	$S_{11}=5\omega-\varepsilon-\theta_1-\theta_2-\gamma_1-\gamma_2$
Species description	Symmetry coordinate[a]
CH_2 antisymmetric stretch	$S_1=r_1-r_2$
CH_2 symmetric stretch	$S_2=r_1+r_2$
CH stretch	$S_3=r_3$
Si–H stretch	$S_4=T$
C=C stretch	$S_5=R_z$
CH_2 deformation	$S_6=2\alpha-\beta_1-\beta_2$
CH in-plane bend	$S_7=\psi_1-\psi_2$
CH_2 wag	$S_8=\beta_1-\beta_2$
CH_2 twist	$S_8=\mu$
CH_2 wag	$S_{10}=\xi_1$
SiH in-plane bend	$S_{11}=5\omega-\varepsilon-\theta_1-\theta_2-\gamma_1-\gamma_2$
SiH bend	$S_{12}=\theta_1-\theta_2-\gamma_1+\gamma_2$
Si–C stretch	$S_{13}=R_1$
$SiCl_2$ antisymmetric stretch	$S_{14}=r_4-r_5$
CH out-of-plane bend	$S_{15}=\xi_2$
$SiCl_2$ symmetric stretch	$S_{16}=r_4+r_5$
Si–C=C bend	$S_{17}=2\pi-\psi_1-\psi_2$
$SiCl_2$ wag	$S_{18}=\gamma_1+\gamma_2-\theta_1-\theta_2$
$SiCl_2$ deformation	$S_{19}=4\varepsilon-\theta_1-\theta_2-\gamma_1-\gamma_2$
$SiCl_2$ rock	$S_{20}=\theta_1-\theta_2+\gamma_1-\gamma_2$
Asymmetric torsion	$S_{21}=\tau$

[a] Not normalized; S_9, S_{10}, S_{12}, S_{14}, S_{15}, S_{20} and S_{21} belong to the A″ symmetry block for the *cis* conformer.

experimental values whereas the predicted Raman spectrum below 1000 cm^{-1} is in reasonable agreement with the observed spectrum. The predicted spectrum is quite useful for making the vibrational assignments for both conformers.

Infrared intensities were also calculated based on the dipole moment derivatives with respect to the Cartesian coordinates. The derivatives were taken from the ab initio calculations at the MP2/6-31G(d) level and transformed to normal coordinates by:

$$\left(\frac{\partial\mu_u}{\partial Q_i}\right)=\sum_j\left(\frac{\partial\mu_u}{\partial X_j}\right)L_{ij}$$

where the Q_i is the ith normal coordinate, X_j is the jth Cartesian displacement coordinate, and L_{ij} is the transformation matrix between the Cartesian displacement coordinates and normal coordi-

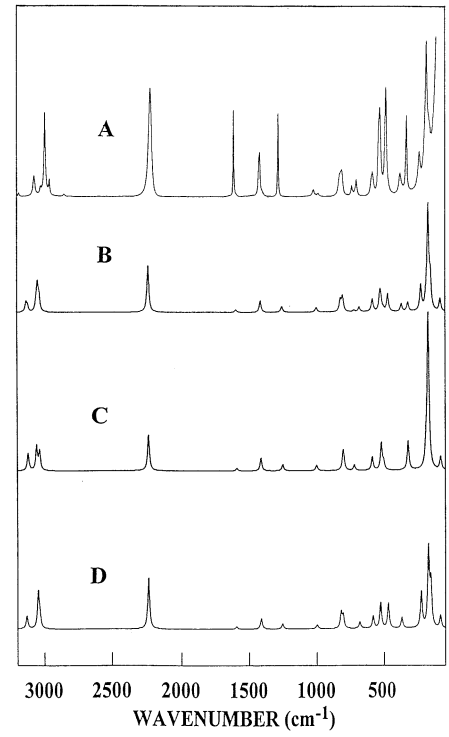

Fig. 5. Predicted and observed Raman spectra of vinyldichlorosilane (A) observed spectrum of liquid (B) predicted spectrum of mixture of *gauche* and *cis* conformers with $\Delta H=20$ cm^{-1} (C) predicted spectrum of pure *cis* conformer (D) predicted spectrum of pure *gauche* conformer.

Table 4
Observed and calculated frequencies (cm^{-1}) for vinyidichlorosilane

Species vib. no.	Fundamentals	*Gauche*							*Cis*						
		Ab initio[a]	Fixed scaled[b]	IR int.[c]	Raman act.[d]	dp ratio[d]	Obs.[e]	P.E.D.[f]	Ab initio[a]	Fixed scaled[b]	IR int.[c]	Raman act.[d]	dp ratio[d]	Obs.[e]	P.E.D.[f]
ν_1	CH_2 antisymmetric stretch	3300	3131	5.0	58.8	0.65	3079	$99S_1$	3289	3120	7.2	76.1	0.60	3074	$98S_1$
ν_2	CH_2 symmetric stretch	3212	3047	4.4	155.2	0.14	3001	$74S_3$, $26S_2$	3199	3035	6.0	78.2	0.15	2965	$96S_3$
ν_3	CH stretch	3199	3035	2.4	45.7	0.72	2965	$74S_2$, $26S_3$	3222	3057	0.4	102.6	0.28	3030	$94S_2$
ν_4	Si–H stretch	2361	2240	126.6	134.7	0.15	2218	$100S_4$	2360	2239	104.8	92.1	0.14	2219	$100S_4$
ν_5	C=C stretch	1679	1593	9.1	4.0	0.16	1603	$62S_5$, $31S_6$	1674	1588	13.9	3.9	0.19	1603	$60S_5$, $34S_6$
ν_6	CH_2 deformation	1486	1410	22.6	14.7	0.43	1413	$69S_6$, $24S_5$	1485	1409	25.2	16.9	0.37	1407	$65S_6$, $27S_5$
ν_7	CH in-plane bend	1321	1253	1.3	6.0	0.35	1272	$62S_7$, $25S_8$	1316	1249	1.3	4.9	0.34	1272	$59S_7$, $26S_8$
ν_8	CH_2 wag	1053	999	18.5	3.5	0.66	1004	$63S_8$, $29S_7$	1054	1000	12.5	4.5	0.67	1004	$61S_8$, $30S_7$
ν_9	CH_2 twist	1049	995	32.5	0.0	0.53	997	$60S_9$, $26S_{15}$, $13S_{10}$	1049	996	27.5	0.0	0.75	997	$64S_9$, $28S_{15}$
ν_{10}	CH_2 wag	1006	954	20.7	0.2	0.74	977	$87S_{10}$	1003	951	29.8	0.1	0.75	973	$92S_{10}$
ν_{11}	SiH in-plane bend	867	822	225.8	11.1	0.74	824	$43S_{11}$, $27S_{12}$, $14S_{20}$, $11S_{18}$	842	799	181.3	6.2	0.68	810	$70S_{11}$, $24S_{18}$
ν_{12}	SiH bend	849	806	177.0	8.5	0.68	810	$36S_{12}$, $24S_{11}$, $19S_{20}$	848	805	200.2	9.5	0.75	810	$66S_{12}$, $32S_{20}$
ν_{13}	Si–C stretch	719	682	24.2	3.6	0.56	694	$69S_{13}$	759	721	62.2	3.0	0.44	730	$76S_{13}$
ν_{14}	$SiCl_2$ antisymmetric stretch	614	583	151.8	5.6	0.73	589	$89S_{14}$	618	587	173.9	6.0	0.75	589	$74S_{14}$, $11S_{15}$
ν_{15}	CH out-of-plane bend	556	527	55.3	10.2	0.36	536	$30S_{15}$, $31S_{16}$, $17S_{18}$, $15S_9$	528	502	0.1	2.5	0.75	(505)	$44S_{15}$, $25S_{14}$, $23S_9$
ν_{16}	$SiCl_2$ symmetric stretch	495	469	13.4	8.5	0.14	482	$57S_{16}$, $19S_{15}$, $10S_9$	547	519	60.6	10.2	0.08	531	$78S_{16}$
ν_{17}	Si–C=C bend	387	367	6.5	2.6	0.62	371	$59S_{17}$, $10S_{18}$, $10S_{20}$	334	318	3.0	5.5	0.24	322	$42S_{17}$, $23S_{18}$, $16S_{16}$, $12S_{13}$
ν_{18}	$SiCl_2$ wag	233	221	4.1	3.9	0.60	226	$35S_{18}$, $20S_{11}$, $16S_{19}$	194	184	5,0	1.4	0.75	(189)	$25S_{18}$, $36S_{17}$, $20S_{19}$, $17S_{11}$
ν_{19}	$SiCl_2$ deformation	176	167	4.5	5.3	0.75	175	$80S_{19}$, $13S_{18}$	179	170	7.3	3.7	0.75	175	$74S_{19}$, $19S_{18}$
ν_{20}	$SiCl_2$ rock	156	149	0.4	2.5	0.73	(156)	$44S_{20}$, $30S_{12}$, $19S_{17}$	174	166	0.2	7.4	0.75	(175)	$55S_{20}$, $26S_{12}$, $10S_{21}$
ν_{21}	Asymmetric torsion	77	77	0.3	6.4	0.75	(103)	$90S_{21}$	75	74	0.0	6.9	0.75	(103)	$85S_{21}$

[a] Calculated with the MP2/6-31G(d) basis set.
[b] Scaling factors of 0.9 for stretching and bending coordinates and 1,0 for torsional coordinates.
[c] Calculated infrared intensities in Km mol^{-1}.
[d] Calculated Raman activities in $Å^4$ amu^{-1}, using RHF/6-31G* basis set.
[e] Frequencies are taken from the infrared spectrum of the gas, except the ones in parentheses, which are taken from the infrared spectrum of the solid.
[f] For a description of the symmetry coordinates see Table 3.

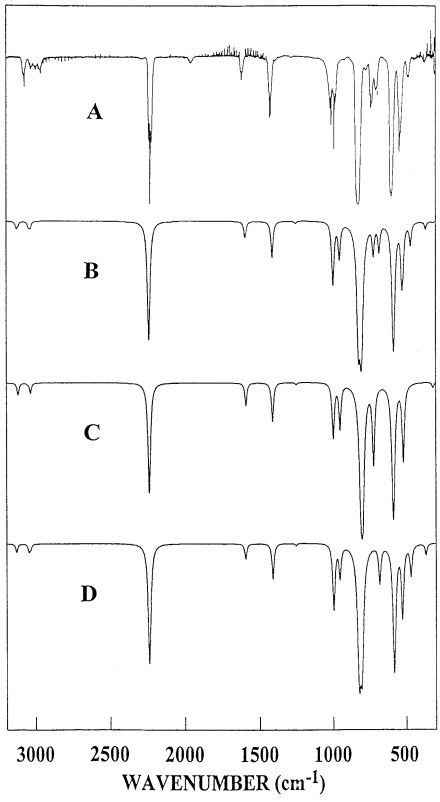

Fig. 6. Predicted and observed infrared spectra of vinyldichlorosilane (A) observed spectrum of gas (B) predicted spectrum of mixture of *gauche* and *cis* conformers with $\Delta H = 20\ cm^{-1}$ (C) predicted spectrum of pure *cis* conformer (D) predicted spectrum of pure *gauche* conformer.

nates. The infrared intensities were then calculated by:

$$I_i = \frac{N\pi}{3c^2}\left[\left(\frac{\partial \mu_x}{\partial Q_i}\right)^2 + \left(\frac{\partial \mu_y}{\partial Q_i}\right)^2 + \left(\frac{\partial \mu_z}{\partial Q_i}\right)^2\right]$$

In Fig. 6C and D, the predicted infrared spectra of the *cis* and *gauche* conformers, respectively, are shown. The combination of the spectra of the two conformers with a ΔH of 20 cm^{-1} is shown in Fig. 6B and the experimental spectrum of the sample in gas phase is shown in Fig. 6A for comparison. These spectra were very useful for selecting the conformer bands for the variable temperature infrared studies.

4. Conformational stability

The determination of the conformational stability is not straightforward because most of the fundamentals of the two conformers are predicted to be near coincident. Nevertheless, it is clear from the spectral data that conformers are present in the fluid phases. The ab initio calculations indicate that the band at 730 cm^{-1} is due to the *cis* conformer where the Si–C stretch, $\nu_{13'}$ is predicted at 721 cm^{-1}. Similarly, the 695 cm^{-1} band is assigned as the corresponding Si–C stretch for the *gauche* conformer with a predicted frequency of 682 cm^{-1}. In the region of 180–400 cm^{-1} there are two fundamentals predicted, ν_{17} and ν_{18}, whereas four bands are observed in this region at 378, 325, 232 and 189 cm^{-1} in the infrared spectrum of the amorphous solid. The corresponding Raman bands are also observed in the spectrum of the amorphous solid phase at 374, 323, 229 and 187 cm^{-1}. Two of these four bands belong to the *gauche* conformer and they are assigned at 374 and 229 cm^{-1} for ν_{17} and ν_{18}, respectively. However, the other two frequencies observed at 323 and 187 cm^{-1} must belong to the *cis* conformer for the corresponding modes as predicted from the MP2/6-31G(d) ab initio calculations. These two bands would not be expected in the solid phase for the less stable conformer but due to the difficulty in obtaining a pure crystalline sample they remain in the amorphous solid.

The conformer pair at 730/695 cm^{-1} was used to determine the enthalpy difference between the conformers from the temperature dependent infrared spectra of the krypton solution. The spectral changes are shown in Fig. 7 and from these data, the increase in the intensity of the infrared band assigned to the *gauche* conformer as the temperature decreases confirms the stability of the *gauche* form over the *cis* conformer in the krypton solution. In order to obtain the enthalpy difference, ten sets of spectral data were obtained for these bands over the temperature range -105 to -150°C (Table 5). The intensity data for the conformer pair were fit to the van't Hoff equation, $-\ln K = (\Delta H/RT) - (\Delta S/R)$, where K is the intensity ratio (I_{cis}/I_g), and it was assumed the ΔH is not a function of temperature. Using a least

squares fit and the slope of the van't Hoff plot, a ΔH value of 20 ± 5 cm^{-1} (235 ± 59 J mol^{-1}) was obtained. This value should be near the value for the gas [19–23] because both conformers have similar sizes and comparable polarities.

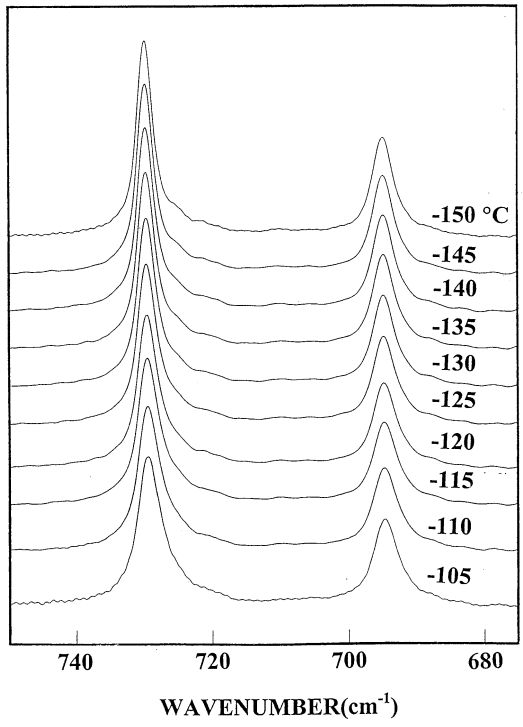

Fig. 7. Temperature dependence of 730 and 695 cm^{-1} infrared bands of vinyldichlorosilane dissolved in liquid krypton.

Table 5
Temperature and intensity ratios for the conformational study of vinyldichlorosilane[a]

T (°C)	1000/T (K)	$I_{730(cis)}/I_{695(gauche)}$	$-\ln K$
−105	5.95	1.9496	−0.6676
−110	6.13	1.9496	−0.6676
−115	6.32	2.0164	−0.7013
−120	6.53	1.9722	−0.6792
−125	6.75	1.9368	−0.6610
−130	6.99	1.9138	−0.6491
−135	7.24	1.8987	−0.6412
−140	7.51	1.8612	−0.6212
−145	7.80	1.8685	−0.6251
−150	8.12	1.8873	−0.6352

[a] $\Delta H = 20 \pm 5$ cm^{-1} (235 ± 58.7 J mol^{-1}) with the *gauche* conformer the more stable form.

5. Vibrational assignment

The vibrational analysis of vinyldichlorosilane is based on the presence of two stable conformations even in the amorphous solid. The *cis* conformer has a plane of symmetry and its 21 normal modes are classified by the symmetry species (A′ and A″) of the C_s symmetry group. The 14A′ modes should produce polarized Raman lines and A, C or A/C-type infrared band contours. The A″ modes should give rise to depolarized lines in the Raman spectrum of the fluid phase and yield B-type infrared band envelop. The *gauche* conformer has only the trivial C_1 symmetry and all the 21 vibrations should yield polarized Raman bands and hybrid A/B/C type infrared band envelopes. Guided by these considerations, the calculated spectral intensities, normal coordinate analysis and the vibrational analysis of the similar molecule vinylchlorosilane [9] the proposed assignments of the observed bands in the infrared and Raman spectra of vinyldichlorosilane are given in Table 1.

The assignment of the carbon-hydrogen modes of the vinyl group is similar to the corresponding modes in chlorovinylsilane [9] with only minor frequency shifts. In fact, the spectra of these two compounds are remarkably similar down to ~ 1000 cm^{-1}. The $=CH_2$ antisymmetric stretch is observed as an A/C-type band at 3074 cm^{-1} in the infrared spectrum of the gas which corresponds to 3071 cm^{-1} in the monochloro [9] compound. The corresponding symmetric mode (ν_3) is observed at 2965 cm^{-1} in the infrared spectrum of the gas and it is observed at the same location at 2965 cm^{-1} in chlorovinylsilane [9]. The =CH stretch is observed as a B-type band centered at 3001 cm^{-1} whereas the same mode is observed at 2993 for chlorovinylsilane [9]. The C=C stretch is observed as an A-type band at 1603 cm^{-1} and the corresponding mode for chlorovinylsilane-d_0 and Si-d_2 is observed at 1600 cm^{-1} for both molecules. However, the Si–H stretch is shifted to higher frequency from 2194 and 2188 for the monochloro molecule to 2219 cm^{-1} as the number of chlorine atoms are increased on the silicon atom. This observation is identical to that found for the corresponding modes in chlorocyclopropy-

lsilane (2193 and 2186 cm^{-1}) and dichlorocyclopropylsilane (2216 cm^{-1}). The four bending modes of the CH_2 group of vinyldichlorosilane are observed at 1413, 1004, 997 and 977 cm^{-1} in the infrared spectrum of the gas with the corresponding modes being observed basically at the same frequencies for chlorovinylsilane [9] at 1411, 1008, 1003 and 960 cm^{-1} for the *gauche* conformer. Three of these four bands for the vinyldichlorosilane molecule are found to be split in the infrared spectrum of the krypton solution but for the chlorovinylsilane molecule the splitting of the corresponding modes could not be observed in the xenon solution. Nevertheless, these comparisons of frequencies for many of the remaining modes for these two molecules can be extended so there is little difficulty in assigning the bands for the remaining fundamentals for both conformers. The heavy atom skeletal bends show large splittings between the corresponding modes for the two conformers.

6. Discussion

It has been determined that the gauche conformer is the more stable rotamer in the rare gas from the temperature study of the infrared spectrum of krypton solution. Utilizing two peaks, which are reasonably separated, one obtains an average enthalpy value of 20 ± 5 cm^{-1} (235 ± 59 J mol^{-1}) in liquified krypton for the one well separated pair. It is believed that this value should be near the value for the vapor [19–23]. Additional support for the *gauche* conformer being the more stable rotamer is found in the relative intensity of the infrared bands for the two conformers utilizing the predicted relative values from the ab initio calculations.

Utilizing the isolated Si–H stretching frequencies from vinyldichlorosilane it is possible to calculate the SiH distances (r_0) for the *gauche* and *cis* conformers [24]. Using the frequencies 2219 and 2218 cm^{-1} for the two different Si–H vibrations for the *cis* and the *gauche* conformers, respectively, the Si–H bond distances are calculated to be 1.474 Å for both conformers. However, the predicted Si–H bond distances from the MP2/6-31G(d) calculations are found to be slightly longer (1.476 Å for both conformers) than this experimental value. On the other hand, the predictions from the MP2/6-311 + G(d,p) calculations are shorter with values of 1.467 and 1.465 Å for the *cis* and *gauche* conformers, respectively. In some recent studies on some other silyl compounds [25–27], the predicted Si–H bond distances from the MP2/6-311 + G(d,p) calculations were found to be ~ 0.005 Å shorter than the experimental value. However the MP2/2-31G(d) calculations gave values near the experimental distances so this basis set at this level of calculations will give the best predictions of the experimental silicon–hydrogen bond distances.

The predicted structural parameters for the two conformers are nearly the same except for the C–Si distance, the CCSi angle and the HCSi angle. The C–Si distance is predicted to be 0.005 Å longer in the *gauche* conformer compared to the similar distance in the *cis* rotamer from all the MP2 calculations with all three basis sets. Similarly the CCSi angle is predicted to be 3.5° larger in the *gauche* form than the corresponding angle in the *cis* conformer which can be rationalized on steric interaction of the chlorine atom with the double bond. Steric effects can also be used to rationalize the larger HCSi angle of the *cis* conformer (120.3°) compared with this angle in the *gauche* rotamer (117.5°). These structural differences in the angles lead to significantly different force constants for the two conformers. For example the bending force constant for the CCSi angle (π) has a value of 0.366 mdyn $Å^{-1}$ for the *gauche* form but the corresponding force constants for the *cis* is only 0.300 mdyn $Å^{-1}$. Similarly the force constant for the HCSi angle bend is $\sim 10\%$ larger for the *gauche* conformer than the corresponding force constant for the *cis* form (0.276 vs. 0.252 mdyn $Å^{-1}$). The other force constant, which is significantly larger for the *gauche* conformer, is the one for the bending of the CSiCl angle which has a value of 0.672 mdyn $Å^{-1}$ compared with the value of 0.504 mdyn $Å^{-1}$ for this force constant for the *cis* rotamer. This large difference is primarily the reason the skeleton bending fundamentals having significantly different wavenumbers for the two conformers.

However, most of the other fundamentals for the two conformers have similar wavenumbers, which is consistent with similar force constants for the two rotamers.

The conformational stability of vinyldichlorosilane can be compared with the corresponding three-membered ring molecule, dichlorocyclopropylsilane. The variable temperature studies [10] of the infrared spectra Of c-$C_3H_5SiHCl_2$ dissolved in liquified xenon indicated that the *gauche* form is the more stable conformer in agreement with the ab initio calculations at all levels of the theory explored with electron correlation. This observation is exactly the same as found for chlorovinylsilane study [9] where all levels of ab initio calculations are consistent with the experimental results. Therefore, for these two molecules it appears that the ab initio calculations with these basis sets correctly predict the conformational stability of these types of silyl chloride molecules. However, this observation was not the case for chlorocyclopropylsilane, c-$C_3H_5SiH_2Cl$, and vinyldichlorosilane, $CH_2CHSiCl_2$, where the ab initio calculation is in agreement with the experimental data only with relatively large basis sets. It would be of interest to investigate whether similar agreements with the ab initio predicted and experimental values for the conformer stabilities for the corresponding fluoride molecules, i.e. $CH_2CHSiHF_2$ and c-$C_3H_5SiH_2F$ are found for only large basis sets.

The vibrational assignments for vinyldichlorosilane had not previously been completely reported [6]. However, because it was not possible to obtain the spectrum of a single conformer from the solid, it was difficult to distinguish which bands were due to which conformer. Nevertheless, the ab initio values were used to make the vibrational assignment for the most part. Using a scaling factor of 0.90 for all modes except 1.0 for the asymmetric torsion, the wavenumbers for the fundamentals are predicted from the MP2/6-31G(d) ab initio calculation to be within 2% for both conformers. Therefore, ab initio calculations at this level provide excellent predictions of the wavenumbers for the fundamentals for these types of silyl molecules.

Acknowledgements

JRD acknowledges partial support of these studies by the University of Missouri–Kansas City Faculty Research Grant program.

References

[1] R. Huag, H. Weinmann, B. Yoachim, F. Aldinger, J. Eur. Ceram. Soc. 19 (1999) 1.
[2] V. Belot, R.J.P. Corriu, D. Leclercq, D.H. Mutin, A. Viox, J. Non-Cryst. Solids 176 (1994) 33.
[3] K. Tamura, Y. Mori, Japanese Patent no. 04166942.
[4] B. Boury, RJ.P. Corriu, D. Leclercq, D.H. Muti, J.M. Planneix, A. Vioux, NATO AST, Sec., E, 1992.
[5] B. Boury, L. Carpenter, R.J.P. Corriu, Angew Chem. 102 (1990) 818.
[6] Y. Pentin, Zh. Prilel, Spectiosk. 24 (1976) 870.
[7] M.D. Allendorf, C.F. Melius, J. Phys. Chem. 97 (1993) 720.
[8] T.K. Gounev, J.W. Weston, S. Shen, M. Dakkouri, A. Grunvogel-Hurst, J.R. Durig, J. Phys. Chem. A 101 (1997) 8614.
[9] J.R. Durig, Y.E. Nashed, M.A. Qtaitat, G.A. Guirgis, J. Mol. Struct. (2000) in press.
[10] J.R. Durig, S.W. Hur, M. Dakkouri, A. Grunvogel-Hurst, T.K. Gounev, Chem. Phys. 226 (1998) 125.
[11] F.A. Miller, B.M. Harney, Appl. Spectrosc. 24 (1970) 291.
[12] M.J. Frisch, G.W. Trucks, H.B. Schlegel, P.M.W. Gill, B.K. Johnson, M.A. Robb, J.R. Cheeseman, T.A. Keith, G.A. Petersson, J.A. Montgomery, K. Raghavachari, M.A. AI-Laham, V.G. Zakrzewski, J.V. Ortiz, J.B. Foresman, J. Cioslowski, B.B. Stefanov, A. Nanayakkara, M. Challacombe, C.Y. Peng, P.Y. Ayala, W. Chen, M.W. Wong, J.L. Andres, E.S. Replogle, R. Gomperts, R.L. Martin, D.J. Fox, J.S. Binkley, D.J. Defrees, J. Baker, J.P. Stewart, M. Head-Gordon, C. Gonzalez, J.A. Pople, Gaussian 94 (revision B. 3), Gaussian Inc., Pittsburgh PA, 1995.
[13] P. Pulay, Mol. Phys. 17 (1969) 197.
[14] J.H. Schachtschneider, Vibrational Analysis of Polyatomic Molecules, Parts V, VI, Technical report nos. 231, 57, Shell Development Co., Houston, TX, 1964, 1965.
[15] M.J. Frisch, Y. Yamaguchi, J.F. Gaw, H.F. Schaefer III, J.S. Binkley, J. Chem. Phys. 84 (1986) 531.
[16] R.D. Amos, Chem. Phys. Lett. 124 (1986) 376.
[17] P.L. Polavarapu, J. Phys. Chem. 94 (1990) 8106.
[18] G.W. Chantry, in: A. Anderson (Ed.), The Raman Effect, Ch. 2, vol. 1, Marcel Dekker, New York, 1971.
[19] W.A. Herrebout, B.J. van der Veken, A. Wang, J.R. Durig, J. Phys. Chem. 99 (1995) 578.
[20] W.A. Herrebout, B.J. van der Veken, J. Chem. Phys. 100 (1996) 9671.

[21] M.O. Bulanin, J. Mol. Struct. 19 (1973) 59.
[22] B.J. van der Veken, F.R. DeMunck, J. Chem. Phys. 97 (1992) 3060.
[23] M.O. Bulanin, J. Mol. Struct. 347 (1995) 73.
[24] J.L. Duncan, J.L. Harvie, D.C. McKean, J. Mol. Struct. 145 (1986) 225.
[25] J.R. Durig, Y.E. Nashed, Y. Jin, G.A. Guirgis, J. Mol. Struct. 449 (1998) 1.
[26] T.A. Mohamed, G.A. Guirgis, Y.E. Nashed, J.R. Durig, Struct. Chem. 10 (1999) 333.
[27] G.A. Guirgis, Y.E. Nashed, J.R. Durig, J. Mol. Struct. 510 (1999) 13.